Desalination and Water Treatment
www.deswater.com
doi: 10.1080/19443994.2014.985257

57 (2016) 2616–2625
February

Taylor & Francis
Taylor & Francis Group

Removal of cibacron black commercial dye with heat- or iron-activated persulfate: statistical evaluation of key operating parameters on decolorization and degradation by-products

Zacharias Frontistis[a], Eduard Martí Mestres[a,b], Ioannis Konstantinou[c], Dionissios Mantzavinos[a,*]

[a]*Department of Chemical Engineering, University of Patras, Caratheodory 1, University Campus, GR-6504 Patras, Greece, Tel. +30 2610996137; email: zaxoys@gmail.com (Z. Frontistis), Tel. +34 600827473; email: edumartimestres@gmail.com (E.M. Mestres), Tel. +30 2610996136; Fax: +30 2610969532; email: mantzavinos@chemeng.upatras.gr (D. Mantzavinos)*
[b]*Department of Chemical Engineering, University of Barcelona, C/Martí i Franquès 1, 08028 Barcelona, Spain*
[c]*Department of Environmental & Natural Resources Management, University of Patras, 2 Seferi St., GR-30100 Agrinio, Greece, Tel. +30 2641074186; email: iokonst@upatras.gr*

Received 30 August 2014; Accepted 16 October 2014

ABSTRACT

Sodium persulfate activated by ferrous ions and/or increased temperature to generate sulfate radicals was employed as an oxidant to decolorize cibacron black, a commercial azo dye formulation. The effect of operating conditions, such as dye concentration (10–100 mg/L), oxidant concentration (30–150 mg/L), Fe^{2+} concentration (0–100 mg/L), temperature (25–70°C), and reaction time (2.5–10 min), on the extent of decolorization was evaluated implementing a 2^5 factorial design approach. Of the five parameters tested and their second and higher order interactions, statistically significant were the three individual concentrations as well as the interaction between iron and sulfate concentrations. With the exception of dye concentration whose effect on decolorization was negative, all other important effects were positive and an empirical mathematical model to describe the process was proposed. At the conditions in question, persulfate activation by iron was found to be more effective than that by heat. LC–MS analysis was also employed to identify likely transformation by-products; although individual structures could not be proposed due to the complex nature of the commercial formulation, several peaks corresponding to the original formulation as well as to the reaction intermediates were identified and their concentration–time profiles were followed.

Keywords: Azo dye; Activation; Factorial design; LC–MS; Sulfate radicals

1. Introduction

Industrial processes usually result in the generation of various bioresistant compounds that are present in the resulting wastewaters. Their removal from these industrial effluents is a challenge to the scientific community. A common approach to mitigate the environmental and health impacts of recalcitrant organic compounds is to destroy them by an oxidation or

*Corresponding author.

Presented at the 2nd International Conference on Recycling and Reuse (R&R2014), 4–6 June 2014, Istanbul, Turkey

reduction reaction (redox process), in order to ease their biodegradability.

In this respect, textile manufacturing generates large quantities of wastewaters that need special attention for their treatment and final disposal. Azo dyes and azo derivatives constitute about a half of the global production of synthetic textile dyes, because of their ability of enduring long-term exposure to sunlight, water, and other undesirable conditions [1]. The disposal of dye wastewater is an environmental concern since the associated color is quite noticeable, and some dyes may have carcinogenic and/or teratogenic effects on public health. Decolorization of wastewaters is one of the significant problems as the dye will be visible even at low concentration. Most of the dyes are found to be resistant to normal treatment processes as they are designed to resist chemical and photochemical degradation [2].

In recent years, various efforts are being made to eliminate or effectively remove azo dyes; among them, advanced oxidation processes (AOPs) are viable alternative options for wastewater treatment [3,4]. In recent years, the sulfate radical-AOP has been discussed in the literature as an efficient and affordable process. Sodium persulfate (SPS) ($Na_2S_2O_8$) has recently attracted the attention of the scientific community as a promising source of sulfate radicals because of its moderate cost (i.e. the wholesale price is in the order of 1,000 USD/tn) and its high redox potential (2.01 V [5]). Other advantages of persulfate over other oxidants include the fact that it is solid at ambient temperature, thus facilitating its storage and transport as well as its high stability and aqueous solubility.

Nevertheless, an intrinsic shortcoming is that SPS reacts very slowly with organic molecules in water and therefore, it has to be activated through its conversion to powerful sulfate radicals ($SO_4^{-\cdot}$); this can be done by the action of heat [6], microwaves [7], ultraviolet radiation [4,5,8], and the presence of transition metals such as iron [9,10], cobalt [11], silver [12], and zinc [13]. The formation of sulfate radicals, whose redox potential (2.6 V [10]) is slightly lower than that of hydroxyl radicals, through persulfate activation by iron or heat (i.e. the topic of this work) is given by reactions (1) and (2), respectively:

$$S_2O_8^{2-} + Fe^{2+} \xrightarrow{\text{chemical-activation}} SO_4^{2-} + SO_4^{-\cdot} + Fe^{3+} \quad (1)$$

$$S_2O_8^{2-} \xrightarrow{\text{thermal-activation}} SO_4^{-\cdot} \ (30^\circ C < T < 99^\circ C) \quad (2)$$

In this work, cibacron black (CB), a widely used azo dye, was chosen as a model compound to investigate its degradation by heat- and/or iron-activated persulfate oxidation. The main scope was to evaluate the effect of various operating conditions such as initial CB and SPS concentrations, reaction time, and the level of activation factors (i.e. temperature and iron) on decolorization. Furthermore, an attempt was made to follow CB degradation kinetics and identify by-products by LC–MS analysis.

Various studies [6,9,10,13] have shown that the sulfate radical-driven oxidation of several dyes may strongly be affected by parameters such as the activation temperature, the solution pH, the presence of buffers as well as the concentration of the contaminant and SPS. Moreover, the quality of the water matrix may also affect process efficiency as demonstrated by Grčić et al. [14], who studied the application of various sulfate radical-driven processes to treat simulated dyehouse effluents. In this work, a statistical approach based on a factorial experimental design was implemented to estimate the effect of the operating parameters in a statistically meaningful way. Factorial designs [15–17], as well as similar approaches like the artificial neural networks [18,19] are increasingly being employed in the literature to model the degradation of dyes by various physicochemical and biological means.

2. Materials and methods

2.1. Chemicals

CB, a monochlorotriazine-type reactive dye, is a commercial dye formulation provided by a local textile industry (Epilektos S.A., Region of Sterea, Greece) its dye ingredient, Reactive Black 8, ($C_{19}H_{11}ClN_8Na_2O_{10}S_2$, C.I. number 18207, CAS number 79828-44-7) is shown in Fig. 1. SPS (99+%, CAS number 7775-27-1) and $FeSO_4{\cdot}7H_2O$ (CAS number 7782-63-0) were purchased from Sigma–Aldrich (USA) and used as received. Stock solutions of CB and SPS were made in deionized water and used to prepare the working reaction mixtures.

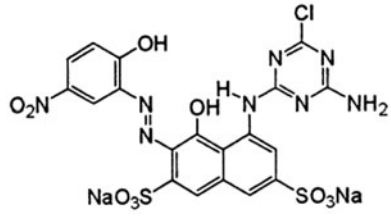

Fig. 1. Chemical structure of the active ingredient of commercial dye formulation.

2.2. Experimental setup

Oxidation reactions were conducted in a 125 mL thermostated reactor made of Pyrex glass. The vessel was open to the atmosphere without gas sparging, since preliminary runs showed that the effect of aeration on degradation was negligible. Certain volumes of CB and SPS stock solutions were mixed to a predefined volume of deionized water in order to get the desired concentration of each reactant (i.e. $[CB]_0 = 10–100$ mg/L; $[SPS]_0 = 30–150$ mg/L). For thermal activation experiments, SPS was added after the working CB solution had reached the desired temperature (i.e. up to 70°C). The solution pH was un-buffered starting from about 6.6 and gradually decreasing to about 4.4, and pH was measured with a pH/ion meter (Mettler Toledo). In those experiments where iron was employed, the appropriate amount of $FeSO_4{\cdot}7H_2O$ was added in the reaction mixture at an initial pH value of 3 which remained nearly unchanged throughout the reaction. All experiments were performed by un-buffered samples periodically drawn from the reactor, which were immediately cooled down at 4°C in an ice bath for about 5 min to quench the reaction and then analyzed to assess (i) the extent of decolorization that had occurred and (ii) the degradation of CB and the possible formation of by-products.

2.3. Analytical

2.3.1. Color removal

CB decolorization was monitored using a DR 5000 UV–vis spectrophotometer (Dr Lange) at 600 nm and a path length of 1 mm. Full scan measurement was also carried out in the range 200–700 nm in order to better understand CB transformation in terms of wavelength and absorbance shifts thereby confirming potential changes of its chemical structure.

2.3.2. LC–MS analysis

An ultra performance liquid chromatography–electrospray ionization–mass spectrometry (UPLC–ESI–MS) system including an Accela Autosampler, an Accela LC pump, and a LTQ orbitrap mass spectrometer (Thermo Fisher Scientific, Germany) was used for the monitoring of degradation kinetics and the identification of CB degradation by-products. ESI–MS analyses were acquired in both positive and negative modes. A C18 Hypersil Gold column (100 × 2.1 mm i.d., 1.9 μm particle size, Thermo Fisher Scientific) was used at 40°C. Injection volume was 10 μL, and flow rate was 300 μL/min. Gradient mobile phase composition was adopted using water/5 mM ammonium formate as solvent A and methanol/5 mM ammonium formate as solvent B with the following program: 90/10 at starting time; 75/25 at 0.5 min; 50/50 at 6 min; 0/100 at 10 min; and then return to 90/10. The ESI-source parameters were as follows: sheath and auxiliary gas flow rate were 35 and 10 (nitrogen, arbitrary units), respectively; source voltage at 3.70 kV; capillary temperature at 320°C. For fragmentation study, the voltage of the HCD collision cell was set at 35 eV. Prior to analysis, the orbitrap mass analyzer was externally calibrated to obtain mass accuracy with ±5 ppm. The analysis was performed using a resolving power of 60,000. UPLC–ESI–MS system was controlled with Xcalibur software version 2.1. Blank methanol samples analyzed before and after the persulfate oxidation samples helped us to target the peaks arising from the treated samples.

3. Results and discussion

3.1. Effect of operating conditions

There are two ways one can investigate the effect of a large number of variables. The most commonly used method involves the variation of one variable while keeping the other variables constant, until all variables have been studied. This methodology has two disadvantages: first, a large number of experiments are required and second, it is likely that the combined effect of two or more variables may not be identified. In this work, a statistical approach was chosen based on a factorial experimental design that would allow us to infer about the effect of the variables with a relatively small number of experiments [20]. The independent variables of the experimental design are presented in Table 1. Each one of the five variables received two values, a high value (indicated by the plus sign) and a low value (indicated by the

Table 1
Range of the factorial design input variables used in this work

Level of value	CB (mg/L)	SPS (mg/L)	Temperature (°C)	Fe^{2+} (mg/L)	Reaction time (min)
−	10	30	25	0	2.5
+	100	150	70	100	10

minus sign). The range of these parameters was chosen on the basis of preliminary experiments.

The experimental design followed in this work was a full 2^5 experimental set, which required 32 experiments plus three additional experiments at the center of the design in order to calculate the standard error and to check the system for non-linear behavior (curvature). The order in which each experiment was performed was selected randomly and is shown in Table 2, along with the values of the independent variables for each run. Table 2 also shows the response (or depended variable) in terms of decolorization at 600 nm. Estimation of the average effect, the main effects (i.e. the effect of each individual variable on the response) and the two and higher order interactions, was made by means of the statistical package Minitab 16; the results are presented in Table 3. To assess the significance of the effects, an estimate of the standard error is required which is usually made by performing repeat runs. In this work, three replicate experiments were performed (i.e. 33–35 in Table 2) at the center of the design [21]. The standard error is then the square root of the variance (half this amount for the average). If an effect is about or below the standard error, it may be considered insignificant (or in other terms, not different from zero). The contribution of a variable,

Table 2
Design matrix of the 2^5 factorial experimental design and observed response

	Level value of each variable in the experimental run					Response	
Order of running experiments	CB	SPS	Temperature	Fe^{2+}	Reaction time	Extent of decolorization	Fitting
31	−	+	+	+	+	0.977	0.988
1	−	−	−	−	−	0.044	0.055
6	+	−	+	−	−	0	0.011
23	−	+	+	−	+	0.646	0.657
24	+	+	+	−	+	0.0542	0.065
21	−	−	+	−	+	0.428	0.439
29	−	−	+	+	+	0.524	0.535
28	+	+	−	+	+	0.736	0.747
5	−	−	+	−	−	0.154	0.165
30	+	−	+	+	+	0.006	0.017
17	−	−	−	−	+	0	0.011
20	+	+	−	−	+	0	0.011
11	−	+	−	+	−	0.67	0.178
18	+	−	−	−	+	0	0.011
3	−	+	−	−	−	0.111	0.122
7	−	+	+	−	−	0.246	0.257
9	−	−	−	+	−	0.603	0.614
32	+	+	+	+	+	0.765	0.776
27	−	+	−	+	+	0.94	0.951
22	+	−	+	−	+	0	0.011
2	+	−	−	−	−	0.0131	0.024
10	+	−	−	+	−	0.0462	0.057
26	+	−	−	+	+	0.092	0.103
12	+	+	−	+	−	0.746	0.757
8	+	+	+	−	−	0	0.011
4	+	+	−	−	−	0.01	0.021
25	−	−	−	+	+	0.752	0.763
14	+	−	+	+	−	0	0.011
15	−	+	+	+	−	0.88	0.891
13	−	−	+	+	−	0.256	0.267
16	+	+	+	+	−	0.765	0.776
19	−	+	−	−	+	0.157	0.168
33	0	0	0	0	0	0.487	0.327
34	0	0	0	0	0	0.448	0.327
35	0	0	0	0	0	0.424	0.327

Table 3
Average and main effects of the independent variables, their two and higher order interaction effects of the 2^5 factorial design on decolorization

Effect	Decolorization-value of effect
Average effect	0.3423 ± 0.01
Main effects	
CB	−0.130 ± 0.021
SPS	0.150 ± 0.021
Temperature	0.024 ± 0.021
Fe^{2+}	0.216 ± 0.021
Reaction time	0.048 ± 0.021
Two-factor interactions	
CB × SPS	0.033 ± 0.021
CB × temperature	−0.028 ± 0.021
CB × Fe^{2+}	−0.023 ± 0.021
CB × time	−0.043 ± 0.021
SPS × temperature	0.036 ± 0.021
SPS × Fe^{2+}	0.1130 ± 0.021
SPS × time	0.0050 ± 0.021
Temperature × Fe^{2+}	−0.05 ± 0.021
Temperature × time	0.021 ± 0.021
Fe^{2+} × time	0.004 ± 0.021
Three-factor interactions	
CB × SPS × temperature	−0.021 ± 0.021
CB × SPS × Fe^{2+}	0.063 ± 0.021
CB × SPS × time	−0.005 ± 0.021
CB × temperature × Fe^{2+}	0.043 ± 0.021
CB × temperature × time	−0.018 ± 0.021
CB × Fe^{2+} × time	−0.003 ± 0.021
SPS × temperature × Fe^{2+}	0.027 ± 0.021
SPS × temperature × time	−0.005 ± 0.021
SPS × Fe^{2+} × time	−0.012±0.021
Temperature × Fe^{2+} × time	−0.026±0.021
Four-factor interactions	
CB × SPS × temperature × Fe^{2+}	−0.019 ± 0.021
CB × SPS × temperature × time	0.011 ± 0.021
CB × SPS × Fe^{2+} × time	0.005 ± 0.021
CB × temperature × Fe^{2+} × time	0.019 ± 0.021
SPS × temperature × Fe^{2+} × time	−0.010 ± 0.021
Five-factor interactions	
CB × SPS × temperature × Fe^{2+} × time	0.010 ± 0.021

however, whose effect appears different from zero, is not necessarily very large.

One way to identify the most important effects is to construct the normal probability plot [22], which is shown in Fig. 2. All effects that are small can be explained as white noise, following a normal distribution with a mean of zero. In the normal probability plot, these effects will appear on a straight line. Any

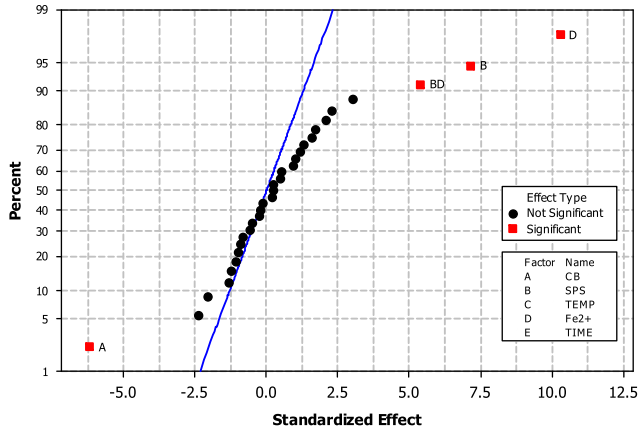

Fig. 2. The normal probability plot.

effects with a significant contribution will lie away from the normal probability line. From all five variables studied, only the concentrations of CB, SPS, and Fe^{2+} appear to have a significant effect on decolorization; with the exception of CB concentration, the effects are positive indicating that an increase in their level brings about an increase in the extent of color removal. The second order interaction between Fe^{2+} and SPS also appears to influence decolorization to a reasonable degree, while other interactions such as temperature × Fe^{2+}, CB × SPS × Fe^{2+} lie close to the normal probability line and their effect may not be substantial. This can evidently be illustrated in Fig. 3, where the effect of all variables and their interactions is shown in the form of the Pareto chart; the ordinate shows the absolute value of the effect, while the abscissa shows the main effects and the interactions. The vertical line shown in Fig. 3 is a reference line indicating the standard error; any effect that extends past this line is potentially significant [20].

Based on the variables and interactions which are statistically significant, a model describing the experimental response was constructed:

$$\%\text{Decolorization} = (0.332 - 0.130\ X_1 + 0.15\ X_2 + 0.215\ X_3 + 0.113\ X_2 \times X_3) \times 100 \quad (3)$$

where X_1, X_2, and X_3 are the transformed forms of the independent variables CB, SPS, and Fe^{2+}, respectively, according to:

$$X_i = \frac{Z_i - \frac{Z_{high}+Z_{low}}{2}}{\frac{Z_{high}-Z_{low}}{2}} \quad (4)$$

and Z_i are the original, untransformed values.

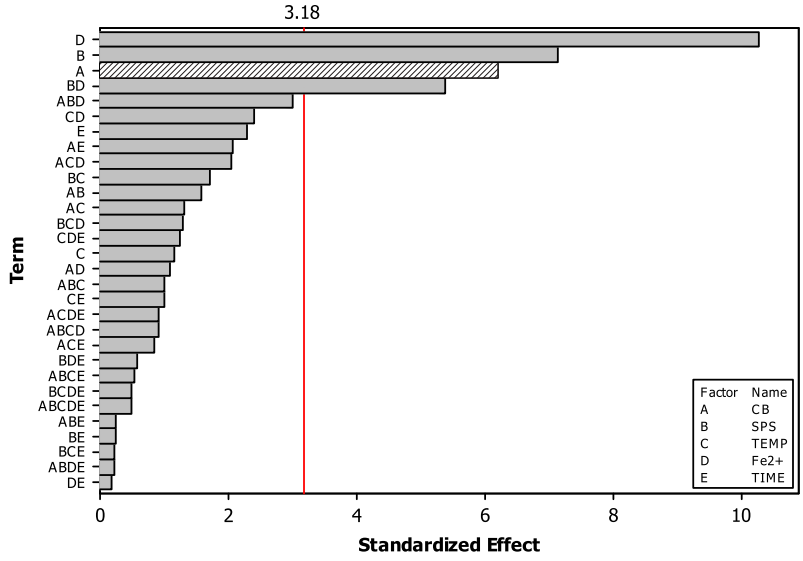

Fig. 3. The Pareto chart. Gray and dashed bars show positive and negative effects, respectively.

Adequacy of the model was also checked by means of constructing the normal plot of the residuals (Fig. 4). Once again, all points from this residual plot lie close to the straight line confirming the conjecture that effects other than those considered in the model may be readily explained by random noise. According to ANOVA analysis there is no evidence of lack of fit ($p \geq 0.1$).

Eq. (3) is a simple mathematical model that can reliably simulate the process within the range of operating conditions that has been developed. This is a good starting point to evaluate process efficiency for a relatively novel treatment system; as already been discussed in the introductory section, there is only one report in the literature regarding the treatment of simulated dye house effluents by the proposed technology [14]. Conversely, the drawback of our approach is that Eq. (3) should be employed with particular caution for conditions outside those it has been developed. For instance, the presence of wastewater constituents, such as chlorine, carbonates, and bicarbonates, all acting as sulfate radical scavengers [14] would decrease decolorization and mineralization kinetics; in this light, a modified factorial design could have been

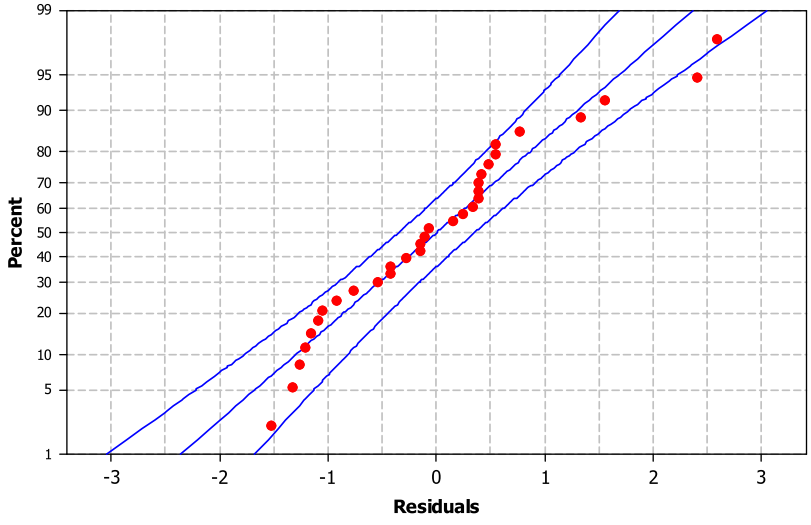

Fig. 4. The normal probability plot of the residuals (95% confidence intervals).

implemented to account for the quality of the water matrix in terms of certain indices (i.e. total organic carbon, conductivity etc.).

3.2. Degradation kinetics and by-products

Some experiments were performed at prolonged reaction times to elucidate degradation kinetics and identify likely by-products. Fig. 5 shows temporal color changes, where at the conditions in question, iron-activated oxidation proceeds substantially faster that the heat-activated one; this is consistent with the findings from the factorial design approach (i.e. iron concentration is a statistically important parameter, while temperature is not). Moreover, this discrepancy becomes more pronounced taking into account that CB concentration, whose effect on color removal is negative, in the iron-activated run is as much as ten times that in the heat-activated one.

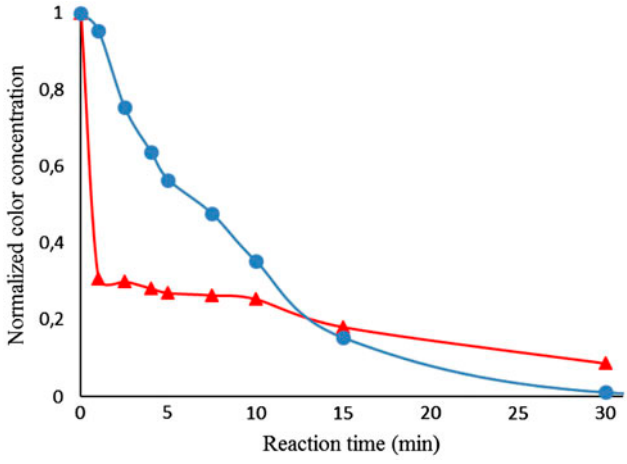

Fig. 5. Normalized color–time profiles during oxidation with 150 mg/L SPS.
Notes: Heat-activated oxidation (circles): CB = 10 mg/L; T = 70°C; and Fe^{2+} = 0 mg/L. Iron-activated oxidation (triangles): CB = 100 mg/L; T = 25°C; and Fe^{2+} = 100 mg/L.

LC–MS analysis led to the identification of five peaks (denoted as P) in the original, unoxidized CB samples whose retention times and m/z values are shown in Table 4. In addition to this, six other peaks (denoted as BP) were also identified as possible transformation by-products accompanying the oxidative degradation of commercial dye formulation. Fig. 6 shows the LC–MS (ESI-) chromatographic profiles for the samples taken at different time intervals during the persulfate oxidation as well as blank methanol sample. The concentration–time profiles (in terms of chromatographic peak areas) of all the identified peaks are depicted in Fig. 7. Parent peaks (i.e. all peaks in Fig. 7(a) and peak at 11.37 min retention time in Fig. 7(c)) decrease readily within 5–10 min of reaction and this is consistent with the decolorization kinetic profiles shown in Fig. 5; on the other hand, peaks at 2.33, 5.18, 5.24, and 7.18 min retention time exhibit the typical pattern of reaction intermediates whose concentration reaches a maximum and then decreases, while peaks at 2.15 and 3.1 min appear to correspond to secondary intermediates formed at later stages of the reaction. All parent compounds and by-products formed at the initial reaction stages were almost totally degraded after 15 min of treatment. These preliminary results on the identification of by-products would be completed with further experiments using an analytical standard of the dye and complementary mass spectrometry, and other analytical techniques.

Table 4
LC–MS data of CB commercial dye constituents and their transformation by-products during heat-activated persulfate oxidation

Retention time (R_t, min)	MS Mode	Parent (P)/By-product (BP)	m/z Base peak (z value)	m/z ion fragments (z value)
11.37	(+)	P	610.1835	353.2662 (1); 348.3116 (1)
7.18	(+)	BP	679.5112 (1) 340.2599 (2)	–
5.24	(+)	BP	475.3243 (1)	453.3428 (1)
8.09	(−)	P	517.9166 (1)	519.9163 (1); 521.9128 (1)
6.22	(−)	P	352.4985 (2)	352.9995 (2); 353.4972 (2)
4.77	(−)	P	471.9562 (1)	–
3.77	(−)	P	523.9767 (1)	497.3339 (1)
5.18	(−)	BP	514.3240 (1)	497.3339 (1); 487.3054 (1)
3.1	(−)	BP	400.4740 (2)	411.4649 (2)
2.33	(−)	BP	450.4656 (2)	410.4872 (2); 461.4564 (2)
2.15	(−)	BP	449.4579 (2)	409.4795 (2); 460.4487 (2)

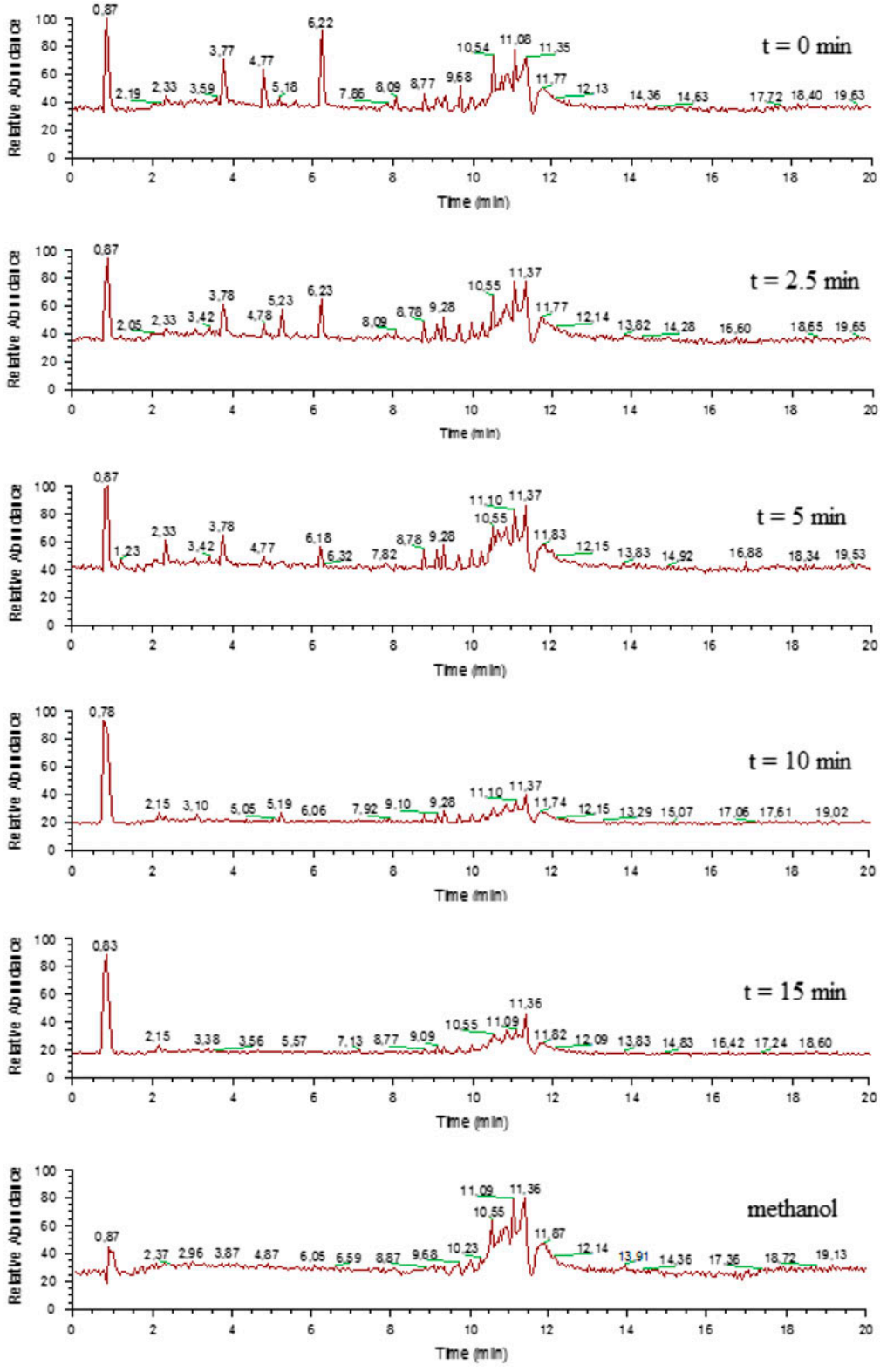

Fig. 6. LC–MS (ESI-) chromatographic profiles of the samples taken at different time intervals ($t = 0$, 2.5, 5, 10, and 15 min) during the persulfate oxidation as well as blank methanol sample.

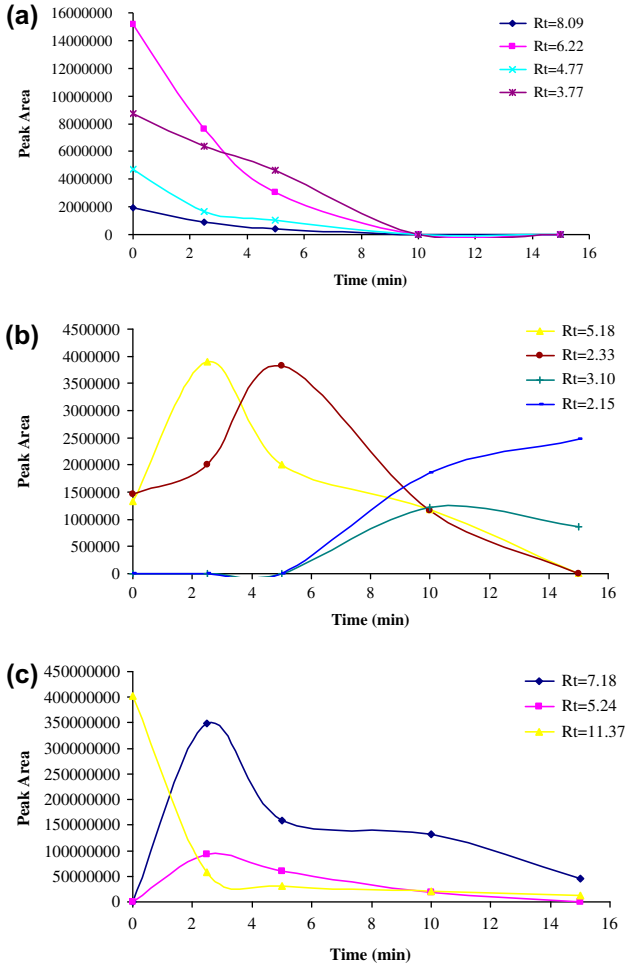

Fig. 7. Concentration–time profiles (in terms of peak areas) of CB constituents and their by-products identified by LC–MS in (a), (b) negative and (c) positive ESI mode during heat-activated persulfate oxidation. Experimental conditions as in Fig. 5.

4. Conclusions

The following conclusions are drawn from this study regarding the heat- and/or iron-activated persulfate oxidation of a commercial dye formulation:

(1) Color removal is affected at a statistically significant level by the dye, persulfate, and iron concentrations as well as the second order interaction of iron and persulfate. All factors but initial dye concentration have a positive effect on the extent of decolorization.

(2) A simple mathematical model can adequately simulate quantitatively decolorization as a function of the most significant main effects and two-factor interactions. It should be pointed out that such models may be meaningful only for the range of conditions within which they have been developed.

(3) Detection of transformation by-products by LC–MS analysis is proved to be a difficult task, since the tested dye is a commercial formulation rather than a pure compound. Several peaks corresponding to the constituents of the dye formulation and reaction intermediates were positively identified but certain structures could not be safely proposed.

Acknowledgments

The authors would like to thank the Unit of Environmental, Organic, and Biochemical high resolution analysis-orbitrap-LC–MS analysis of the University of Ioannina for providing access to the facilities.

References

[1] H. Zhang, L. Duan, D. Zhang, Decolorization of methyl orange by ozonation in combination with ultrasonic irradiation, J. Hazard. Mater. 138 (2006) 53–59.

[2] Q. Liu, Z. Zheng, X. Yang, X. Luo, J. Zhang, B. Zheng, Effect of factors on decolorization of azo dye methyl orange by oxone/natural sunlight in aqueous solution, Environ. Sci. Pollut. Res. 19 (2012) 577–584.

[3] I.K. Konstantinou, T.A. Albanis, TiO_2-assisted photocatalytic degradation of azo dyes in aqueous solution: Kinetic and mechanistic investigations, Appl. Catal. B: Environ. 49 (2004) 1–14.

[4] Y. Gao, N. Gao, Y. Deng, Y. Yang, Y. Ma, Ultraviolet (UV) light-activated persulfate oxidation of sulfamethazine in water, Chem. Eng. J. 195 (2012) 246–253.

[5] Y. Lin, C. Liang, J. Chen, Feasibility study of ultraviolet activated persulfate oxidation of phenol, Chemosphere 82 (2011) 1168–1172.

[6] A. Ghauch, A.M. Tuqan, N. Kibbi, S. Geryes, Methylene blue discoloration by heated persulfate in aqueous solution, Chem. Eng. J. 213 (2012) 259–271.

[7] S.Y. Yang, P. Wang, X. Yang, G. Wei, W.Y. Zhang, L. Shan, A novel advanced oxidation process to degrade organic pollutants in wastewater: Microwave-activated persulfate oxidation, J. Environ. Sci. 21 (2009) 1175–1180.

[8] Y.F. Huang, Y.H. Huang, Identification of produced powerful radicals involved in the mineralization of bisphenol A using a novel UV-$Na_2S_2O_8$/H_2O_2-Fe(II, III) two-stage oxidation process, J. Hazard. Mater. 162 (2009) 1211–1216.

[9] S. Rodriguez, L. Vasquez, D. Costa, A. Romero, A. Santos, Oxidation of orange G by persulfate activated by Fe(II), Fe(III) and zero valent iron (ZVI), Chemosphere 101 (2014) 86–92.

[10] H. Kusic, I. Peternel, S. Ukic, N. Koprivanac, T. Bolanca, S. Papic, A. Bozic, Modeling of iron activated persulfate oxidation treating reactive azo dye in water matrix, Chem. Eng. J. 172 (2011) 109–121.

[11] G.P. Anipsitakis, D.D. Dionysiou, Degradation of organic contaminants in water with sulfate radicals generated by the conjunction of peroxymonosulfate with cobalt, Environ. Sci. Technol. 37 (2003) 4790–4797.
[12] G.P. Anipsitakis, D.D. Dionysiou, Radical generation by the interaction of transition metals with common oxidants, Environ. Sci. Technol. 38 (2004) 3705–3712.
[13] H. Li, J. Guo, L. Yang, Y. Lan, Degradation of methyl orange by sodium persulfate activated with zero-valent zinc, Sep. Purif. Technol. 132 (2014) 168–173.
[14] I. Grčić, S. Papić, N. Koprivanac, I. Kovačić, Kinetic modeling and synergy quantification in sono and photooxidative treatment of simulated dyehouse effluent, Water Res. 46 (2012) 5683–5695.
[15] Y.-S. Woo, M. Rafatullah, A.F. Al-Karkhi, T.-T. Tow, Removal of terasil red R dye by using fenton oxidation: A statistical analysis, Desalin. Water Treat. 52 (2014) 4583–4591.
[16] S. Achour, E. Khelifi, L. Ayed, A.N. Helal, A. Bakhrouf, Response surface methodology for textile wastewater decolourization and biodegradation by a novel mixed bacterial consortium developed via mixture design, Desalin. Water Treat. 52 (2014) 1539–1549.
[17] R. Bhatnagar, H. Joshi, I.D. Mall, V.C. Srivastava, Electrochemical treatment of acrylic dye-bearing textile wastewater: Optimization of operating parameters, Desalin. Water Treat. 52 (2014) 111–122.
[18] M. Eskandarian, F. Mahdizadeh, L. Ghalamchi, S. Naghavi, Bio-Fenton process for acid blue 113 textile azo dye decolorization: Characteristics and neural network modeling, Desalin. Water Treat. 52 (2014) 4990–4998.
[19] M.E.M. Ali, T.A. Gad-Allah, E.S. Elmolla, M.I. Badawy, Heterogeneous Fenton process using iron-containing waste (ICW) for methyl orange degradation: Process performance and modeling, Desalin. Water Treat. 52 (2014) 4538–4546.
[20] A. Katsoni, Z. Frontistis, N.P. Xekoukoulotakis, E. Diamadopoulos, D. Mantzavinos, Wet air oxidation of table olive processing wastewater: Determination of key operating parameters by factorial design, Water Res. 42 (2008) 3591–3600.
[21] F. Torrades, J. García-Montaño, Using central composite experimental design to optimize the degradation of real dye wastewater by Fenton and photo-Fenton reactions, Dyes Pigm. 100 (2014) 184–189.
[22] G.E.P. Box, W.S. Hunter, J.S. Hunter, Statistics for Experimenters, Wiley, New York, NY, 1978.